Thermal Desorption of Deuterium from Polycrystalline Nickel Pre-Implanted with Helium

by

San-Qiang Shi, E. Abramov*, D.A. Thompson
Department of Engineering Physics
and W.W. Smeltzer
Department of Materials Science and Engineering
McMaster University, Hamilton, Ontario L8S 4M1
Canada

*Permanent Address: Nuclear Research Center Negev, P.O. Box 9001, Beer-Sheva, ISREAL 84190

Paper presented for publication[1] to the Jrnl of Nuclear Materials

ABSTRACT

The thermal desorption technique has been used to study the trapping of deuterium atoms in high-purity polycrystalline nickel pre-implanted with helium from $1x10^{19}$ to $5x10^{20}$ ions/m^2. The effect of post-implantation annealing at 703K and 923K on the desorption behavior was investigated. Measured values of the total amount of detrapped deuterium (Q_T) and helium concentration were used in a computer simulation of the desorption curve. It was found that the simulation using one or two discrete trap energies resulted in an inadequate fit between the simulated and the measured data. Both experimental and simulation results are explained using a stress-field trapping model. The effective binding energy, E_b^{eff}, was estimated to be in the range of 0.4-0.6 eV. Deuterium charging was found to stimulate a release of helium at a relatively low temperature.

I. Introduction

In fusion reactors, hydrogen isotope trapping and release characteristics will greatly affect fuel recycling and therefore, the tritium inventory in the first-wall, limiter/diverters, and tritium permeation to the coolant.

The most important trapping effect was observed [1,2] to be the result of an interaction between the hydrogen isotopes and the helium impurity which can build up in the first-wall through various processes. To understand the helium effect, extensive investigations have been carried out into the microstructure changes introduced by helium implantation [3,4] and by post-implantation annealing [5-8].

In the present study, we focus on the helium trapping effect by measuring the deuterium desorption rate from nickel pre-implanted with helium. In contrast to most of the previous work, in which the introduction of deuterium after the helium implantation was carried out by ion implantation, thermal charging from deuterium gas was used in the present research. This method enabled a study of the interaction of the dissolved deuterium with the helium and helium induced radiation damage without the production of additional damage created by a deuterium implantation process.

2.Experimental

The samples for the present study were cut from 25 μm thick high purity (99.99 at.%) nickel foils. They were vacuum annealed at 1173K for 20 hrs, prior to the helium implantation. The average grain size obtained after annealing is about 25 μm. The samples were subsequently implanted, at room temperature, with 30 keV He ions to doses varying from $1x10^{19}$ to $5x10^{20}$ atoms/m^2. In order to avoid beam heating effects the sample holder was water cooled and the beam current density maintained at < $5x10^{-3}$ A/m^2. The projected range for 30 keV He ions (R_p) and the range straggling (ΔR_p) were obtained using TRIM 89 [9] and found to be 116 nm and 48.5 nm respectively. Table 1 summarizes the implantation parameters for the present study.

After the helium implantation, some samples were not annealed, while others were vacuum annealed at 703K or at 923K, for 1 hour. The lower annealing temperature of 703K was chosen to enable some short range rearrangement of helium clusters [7]. The higher temperature (923 K) anneals were carried under conditions where helium bubble migration and growth was recently reported by Chernikov et al. [8]. Before thermal desorption, all samples were thermally charged at 423K in deuterium gas at a pressure of 70 torr for 2 hours. To avoid deuterium release during the cool down to room temperature, the samples were quenched using liquid nitrogen.

The thermal desorption measurements are performed in a high vacuum chamber which is pumped with a turbomolecular pump to a

base pressure of ~10^{-8} torr. The sample to be measured is inserted into a heating element core which was carefully designed to provide uniform heating across the sample. The temperature is measured by a chromel-alumel type thermocouple which is inserted into the heating core close to the sample. The temperature difference between the sample and the thermocouple was found to be less than 3K. The temperature ramping is controlled by an accurate, digital controller and a smooth and constant ramping rate is achieved. Ramp rates were 1.5 or 20 K/min from room temperature to as high as 923K.

The deuterium partial pressure is measured using a quadrupole mass spectrometer equipped with an electron multiplier. The deuterium flux measurements are calibrated using two different calibrated deuterium leaks differing by 3 orders of magnitude. Accurate partial pressure measurements can be made down to 10^{-13} torr, which is equivalent to a desorption flux of ~10^{14} deuterium molecules/m^2/s. A microcomputer is used to control the system, as well as to collect and analyze the data.

In order to check the system and the experimental method, reference nickel samples, without helium pre-implantation, were thermally-charged with deuterium and then measured in the desorption system. The results show that aging for about 2 hours at room temperature is sufficient to degas most of the untrapped deuterium atoms which are dissolved in normal interstitial sites. Consequently, the thermal desorption measurements which are described in this article were performed at least 2 hours after the deuterium charging.

3.Thermal desorption

Thermal desorption (TD) is a powerful technique to study diffusion processes [10], gas-surface interactions [11] and trapping effects [12]. However, the analysis of the data to extract the diffusion coefficients and surface or bulk trapping parameters (binding energy and traps densities) is complicated and usually possible only by making some simplifying assumptions. Redhead [11] and Carter [13] developed similar theories to analyze the desorption data during linear or reciprocal temperature variation, but assumed that the released gas atoms are adsorbed on the sample surfaces. Later, Farrell and Carter [10] suggested a model which includes diffusion processes from the bulk. However their model is not suitable when high defect concentrations are present, as in the case of helium implantation.

The common analytical methods for solving diffusion with defect trapping [12, 14, 15] are based on the theory suggested by McNabb and Foster [16] in which a trapping term is added to Fick's second law, and another differential equation to calculate this trapping term is necessary. A computer code DIFFUSE [15], based on this model, is in widespread use. In the present study, we used our own microcomputer based code, DIFFER, which assumes that local equilibrium between hydrogen atoms dissolved in normal interstitial sites and trapping sites is always maintained: ie., the equilibrium trapping theory suggested by Oriani [17] is employed. Although this code is restricted to only two discrete trapping energies, the final results agree well with comparable

calculations obtained using the alternate approach [18].

It should be noted that both DIFFUSE and DIFFER are limited to discrete trapping energies. The disagreement between the measured experimental data and the simulated curves, which result from this limitation, will be discussed later.

4.Results and Discussion

4.1 Desorption data

Figures 1 and 2 present the thermal desorption measurements for the samples which were pre-implanted with 30 keV He^+ to doses of $1x10^{19}$ and $3.5x10^{19}/m^2$ respectively. It is clearly seen that after annealing at both 703K and 923K the total amount of trapped deuterium is significantly reduced. In both cases, but more clearly for the samples containing $1x10^{19}$ He/m^2, the annealing treatments shift the desorption peak to higher temperature and the desorption rate in the high temperature tails exceeds that of the unannealed sample.

The thermal desorption data for the samples which were pre-implanted with $8x10^{19}$ and $5x10^{20}$ He/m^2 are presented in figures 3 and 4 respectively. In both cases, post-implantation annealing at 923K results in a lower temperature onset for the release of trapped deuterium atoms. The same occurs, for the samples implanted with $8x10^{19}$ He/m^2 and annealed at 703K. However, this low temperature release is not seen in the samples, pre-implanted with $5x10^{20}$ He/cm^2 and annealed at 703K.

Table 2 summarizes the trapping efficiency, i.e., the ratios of trapped deuterium to helium atoms. As one can see, for lower

helium doses, the reduction in the trapping efficiency by annealing became more significant.

4.2 Simulation results

As being mentioned earlier, a computer code " DIFFER " has been used to simulate the thermal desorption experiments. In the simulation, the trap density was arbitrarily chosen to be equal to the helium concentration, the total amount of desorption was taken as the measured values (Q_T), and helium depth profile was given using TRIM 89 [9].

Fig.5 shows typical simulation results for 1 and 2 traps compared with the actual desorption measurement for a sample which had been pre-implanted with $5x10^{20}$ He/m^2. Using a single trap the simulated desorption curve (dashed line in Fig.5) is narrower than that measured, resulting a higher peak desorption rate. A 2-trap simulation (solid line in Fig.5) is a better fit but the measured data still extends to higher temperature. Wilson et al. had previously found a similar misfit in stainless steel pre-implanted with helium ions [12] using a different computer code. It should be mentioned that in the simulation here we did not intend to find a best fit to the experimental data but to show how the curve broadens when using two kinds of traps (0.5 and 0.6 eV) with relative trapping densities of 3:2. The misfit will be explained in next section.

In spite of the misfit, however, we estimated an effective binding energy, E_b^{eff} , by setting the peak release temperature (T_p) of a single trap simulation at the temperature corresponding

to the measured temperature at which 50 % of trapped deuterium had been released. Therefore the values of E_b^{eff} obtained in such way have only relative rather than absolute meaning. The estimated values of E_b^{eff} are shown in Table 3. One can see from Table 3 that E_b^{eff} increases after 703 K annealing in the two low dose cases, decreases in the $8x10^{19}He/m^2$ case and is unchanged in the $5x10^{20}He/m^2$ case. Annealing at 923 K decreases E_b^{eff} vs that after 703 K annealing except in the lowest dose case in which it remains unchanged.

4.3 Discussion

In order to understand the experimental results, two questions have to be answered, i.e., what are the helium configurations before and after annealing and what is the trapping mechanism for deuterium to helium defects.

It is believed that He atoms have very low migration energy in normal interstitial sites of nickel (≈ 0.1 eV [19]). Nevertheless, both experimental [7] and theoretical [20] works showed that He atoms can be strongly trapped by radiation induced defects such as vacancies, to form helium-vacancy complexes. The binding energy of He atoms to vacancies and in helium-vacancy complexes varies from 1 eV to more than 3 eV according to the size of He-vacancy complexes. After ion-implantation at room temperature, most of He atoms stay in such complexes. As the implantation dose is increased, more He atoms are formed in He-bubbles rather than in small clusters. In the present study, such bubbles are quite possibly over pressurized because of the

low implantation temperature.[8]

Two basic physical models for the trapping mechanism of deuterium atoms at or near helium bubbles have been suggested. A chemisorption-like trapping mechanism at the bubble surface [21] results in a discrete binding energy for the deuterium atoms adsorbed at the bubble walls. More recently it was suggested [22,23] that deuterium atoms are attracted towards the helium bubbles and trapped by the surrounding stress fields created by the very high pressure inside the bubble. According to the latter model a spatially extending distribution of binding energies exists around a bubble with a maximum occurring at the bubble surface. The stress-field model can be used to explain the current results.

For low dose samples, assuming that a large fraction of the He atoms are in small helium-vacancy complexes after room temperature implantation, one can expect that these complexes or clusters may serve as low energy but high density trapping centers and that some of them may be rearranged to form larger clusters or bubbles during the 703 K anneal. This would be expected to increase the effective binding energy while decreasing the trap density, as shown in Fig.1 and 2.

For the high dose samples ($8x10^{19}$-$5x10^{20}$ He/m^2) a large fraction of the He atoms will be in bubbles or large clusters after the room temperature implantations. According to the Stress Model [22,23], the stress field around such bubbles is a fairly strong trapping field for deuterium. Therefore the effective binding energies should be higher before annealing than for the

low dose samples. For the $8x10^{19}$ He/m^2 dose, the bubbles are expected to be smaller than in the $5x10^{20}He/m^2$ case allowing significant rearrangement during the 703K anneal and stress relaxation resulting in a reduction in E_b^{eff} as seen. By contrast, the larger bubbles formed at the highest dose remain stable during the 703 K anneal leading to no change in E_b^{eff} and a smaller reduction in the total amount of trapped deuterium (Q_T).

Annealing at 923 K releases part of stress around the bubbles (see Fig.2,3,4) through absorption of vacancies supplied by dissociation of vacancy type defects and vacancy diffusion from the free surface. This results in an earlier onset of desorption at ~ 300 K for the high dose samples. The fact that no clear change between 703K annealing and 923K annealing for samples pre-implanted with 10^{19} He/m^2 may be due to the shortage of vacancy sources from radiation defects.

The stress-field trapping model can also be used to explain the difference between the thermal desorption data and the simulation results predicted by DIFFER, using discrete binding energies. Our results support the concept of a distribution of trapping energies. Trapping models based on discrete binding energies may not be appropriate for helium defects. It is also important to point out that some workers [18] simulated the release curves of deuterium from helium pre-implanted samples fairly well, but in these cases the experimental data was based on deuterium retention measurements which are much less sensitive to small changes in the trapping parameter than desorption rate measurements. It is concluded then, that this type of comparison

between experiment and simulation yields, at best, an effective trap energy, whereas in the real case there may be a distribution of trap energies. In the present study the effective trap energies are within the range of 0.4-0.6 eV with the higher values found for the samples implanted to higher helium doses. Similar values of E_b^{eff} were previously calculated based on the stress field trapping model [24].

4.4 The effect of deuterium charging on helium release

Thermal desorption measurements for samples which were implanted with helium, but not charged with deuterium, show that helium release is negligible, even at temperatures as high as 923K. These results agree with other studies in which, for He doses less than $2x10^{21}$ at/m^2, no helium release was observed during a post-implantation thermal desorption [18]. However, in the present study we found that deuterium charging can stimulate helium release at a relatively low temperature. Figure 6 shows a comparison of the thermal desorption data for two samples pre-implanted with $1x10^{19}$ He/m^2; one was charged with deuterium while the second was not charged. In order to detect the small quantity of gas released, the desorption rates were measured during a temperature ramping at a rate of 20K/min. After the deuterium charging a clear peak for helium release is observed with peak temperature at ~600K. Confirmation that the ~600K release is He was achieved by carrying out a desorption experiment after charging the sample with hydrogen. These results indicate that the deuterium atoms interact with the helium clusters or with

the helium-vacancy complexes in a way that reduces the binding energy of helium atoms in those clusters.

5. Conclusions

(a) The thermal desorption technique was used to study the trapping of deuterium atoms in nickel samples pre-implanted with helium to concentrations of 0.09-4.4 at.%.

(b) Post-implantation annealing at 703K generally reduces the trap density. However, for low helium content it increases the peak release temperature probably due to rearrangement of helium clusters and He-vacancy complexes to create small bubbles.

(c) Post-implantation annealing at 923K reduces both the trap density and the effective trap energy. This is believed to occur due to stress relaxation around the helium bubbles.

(d) An attempt to simulate the desorption curve with one or two discrete trap energies suggests that a better approach would be to consider the distribution of trapping energies around helium bubbles, which is consistent with a stress field trapping model.

(e) The effective trap energy, E_b^{eff} is found to be within the range of 0.4 to 0.6 eV, with higher values generally found for the higher helium content samples (up to 4.4 at.%) where most of the helium atoms are in the form of helium bubbles.

(f) Deuterium atoms interact with helium clusters and He-vacancy complexes to reduce the trapping energy of helium atoms such that He release is observed at ~600K.

Acknowledgements

We would like to thank Mr. B. McClelland for the helium-implantations. We would also like to express our gratitude to the Canadian Fusion Fuels Technology Project (CFFTP) and the Natural Sciences and Engineering Research Council of Canada for funding this research.

References

[1] S.M. Myers, D.M. Follstaedt, F. Besenbacher and J. Bøttiger,J. Appl. Phys. 53 (1982) 8734.

[2] K.L. Wilson, A.E. Pontav, L.G. Haggmark, M.I. Baskes, J. Bohdansky and J. Roth, J. Nucl. Mater. 103 & 104 (1981) 493.

[3] P.B. Johnson and D.J. Mazey, Rad. Eff. 13 (1980) 195.

[4] W. Jäger and J. Roth, J. Nucl. Mater. 93&94 (1980) 756.

[5] N. Marochov, L.J. Perryman and P.J. Goodhew, J. Nucl. Mater. 149 (1987) 296.

[6] R.E. Stoller and G.R. Odette, J. Nucl. Mater. 154 (1988) 286.

[7] P. Ehrhart, A. Gaber and W. Jäger, Acta Metall. 35 (1987) 1943.

[8] V.N. Chenikov, H. Trinkaus, P. Jung and H. Ullmaier, J. Nucl. Mater. 170 (1990) 31.

[9] J.F. Ziegler, J.P. Biersack and U. Littmark, The Stopping Range of Ions in Solids (Pergamon press, New York, 1985).

[10] G. Farrel and G. Carter, Vacuum 17 (1967) 15.

[11] P.A. Redhead, Vacuum 12 (1962) 203.

[12] K.L. Wilson and M.I. Baskes, J. Nucl. Mater. 76 & 77 (1978) 291.

[13] G. Carter, Vacuum 12 (1962) 245.

[14] M. Iino, Metall. Trans. 18A (1987) 1559.

[15] M.I. Baskes, Diffuse 83, SNL Report, SAND 83-8231 (June 1983).

[16] A. McNabb and P.K. Foster, Trans. Metall. Soc. A.I.M.E. 227, (1963) 618.

[17] R.A. Oriani, Acta Metall. 18 (1970) 147.

[18] S.M. Myers, P.M. Richards, W.R. Wampler and F. Besenbacher, J. Nucl.. Mater. 165 (1989) 9.

[19] V. Philipps and K. Sonnenberg, J. Nucl. Mater., 114 (1983) 95.

[20] W.D. Wilson, C.L. Bisson and M.I. Baskes, Phys. Rev. B, 24(10) (1981) 5616.

[21] S Myers, Proc. Conf. on Environmental Degradation of Engineering Materials, Blacksburg, VA. (1981) 403.

[22] E. Abramov and D. Eliezer, J. Mat. Sci. Lett. 7 (1988) 108.

[23] E. Abramov and D. Eliezer, Proc. Conf. on the Effects of Hydrogen on Materials Behaviour, Jackson Hole, Wyoming (1989) to be published.

[24] E. Abramov and D. Eliezer, Sci. Met., in press.

Table 1

Implantation Parameters

Dose (He atoms/m^2)	Peak helium concentration (at.%)	Radiation damage (dpa)*
$1x10^{19}$	0.09	0.06
$3.5x10^{19}$	0.31	0.2
$8x10^{19}$	0.70	0.5
$5x10^{20}$	4.4	~ 3.2

* displacements per atom, predicted using TRIM 89 [9].

Table 2

Ratios of trapped Deuterium to Helium in Nickel

He dose (atoms/m^2)	D/He = Q_T/He no anneal	703K anneal	923K anneal
$1x10^{19}$	1.2	0.4	0.4
$3.5x10^{19}$	1.3	0.6	0.3
$8x10^{19}$	1.5	0.84	0.8
$5x10^{20}$	0.64	0.4	0.4

Table 3

The effective binding energy estimated using DIFFER

He dose (atoms/m^2)	no anneal (eV)	703K anneal (eV)	923K anneal (eV)
$1x10^{19}$	0.45	0.52	0.52
$3.5x10^{19}$	0.46	0.51	0.48
$8x10^{19}$	0.56	0.52	0.50
$5x10^{20}$	0.52	0.52	0.50

Figure Captions

Fig.1 Deuterium thermal desorption from nickel pre-implanted with 30 keV He to a dose of $1x10^{19}He/m^2$. Ramp rate = 1.5 K/min.

Fig.2 Deuterium thermal desorption from nickel pre-implanted with 30 keV He to a dose of $3.5x10^{19}He/m^2$. Ramp rate = 1.5 K/min.

Fig.3 Deuterium thermal desorption from nickel pre-implanted with 30 keV He to a dose of $8x10^{19}He/m^2$. Ramp rate = 1.5 K/min.

Fig.4 Deuterium thermal desorption from nickel pre-implanted with 30 keV He to a dose of $5x10^{20}He/m^2$. Ramp rate = 1.5 K/min.

Fig.5 Comparison of simulated deuterium thermal desorption curves using DIFFER with experimental result on nickel pre-implanted with 30 keV He to a dose of $5x10^{20}He/m^2$. Ramp rate = 1.5 K/min. The dashed curve is calculated using a single trap, the solid curve uses two traps with different trap densities.

Fig.6 Helium thermal desorption from nickel samples pre-implanted at 30 keV with $1x10^{19}$ He/m^2, with and without deuterium charging. Ramp rate = 20 K/min.

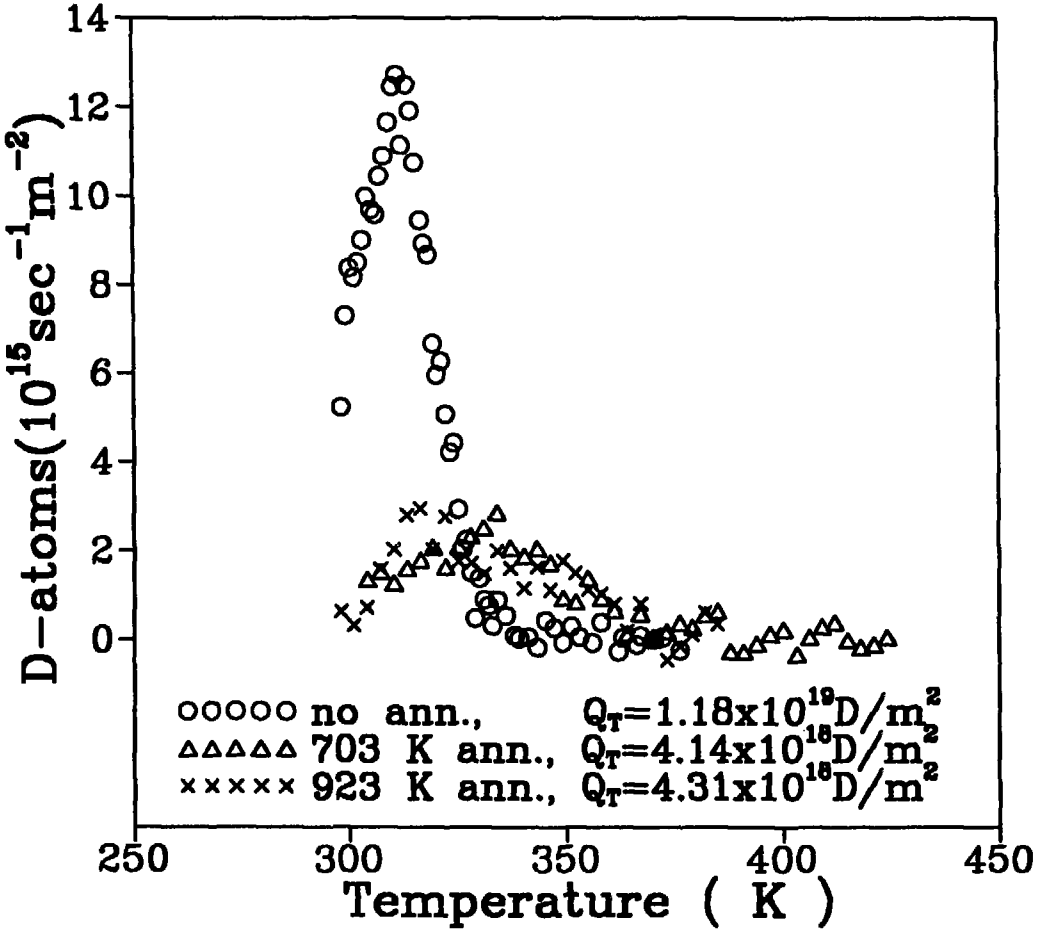
D−atoms(10^{15}sec^{-1}m^{-2})
14
12
10
8
6
4
2
0
250
300
350
400
450
Temperature (K)
○○○○○ no ann., Q_T=1.18x10^{19}D/m^2
△△△△△ 703 K ann., Q_T=4.14x10^{18}D/m^2
×××××× 923 K ann., Q_T=4.31x10^{18}D/m^2

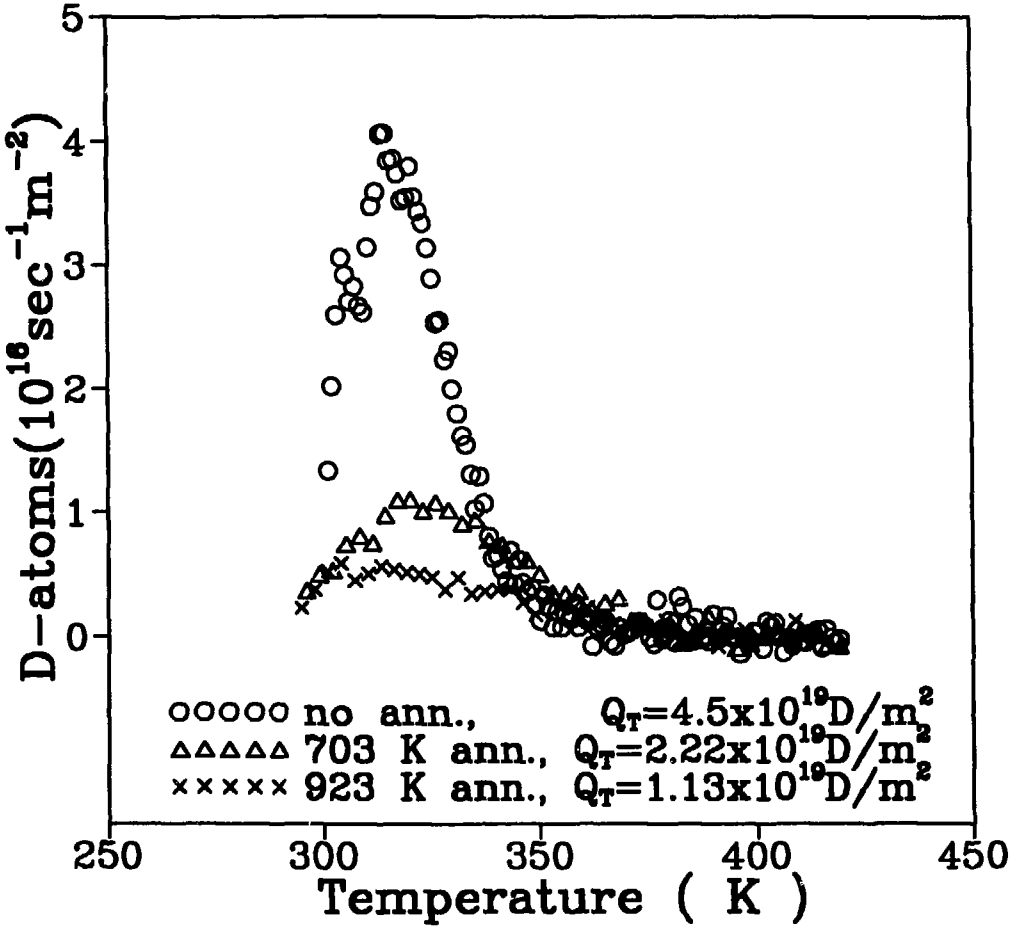
D−atoms(10^{16}sec^{-1}m^{-2})
5
4
3
2
1
0
250
300
350
400
450
Temperature (K)
○○○○○ no ann., Q_T=4.5x10^{19}D/m^2
△△△△△ 703 K ann., Q_T=2.22x10^{19}D/m^2
××××× 923 K ann., Q_T=1.13x10^{19}D/m^2

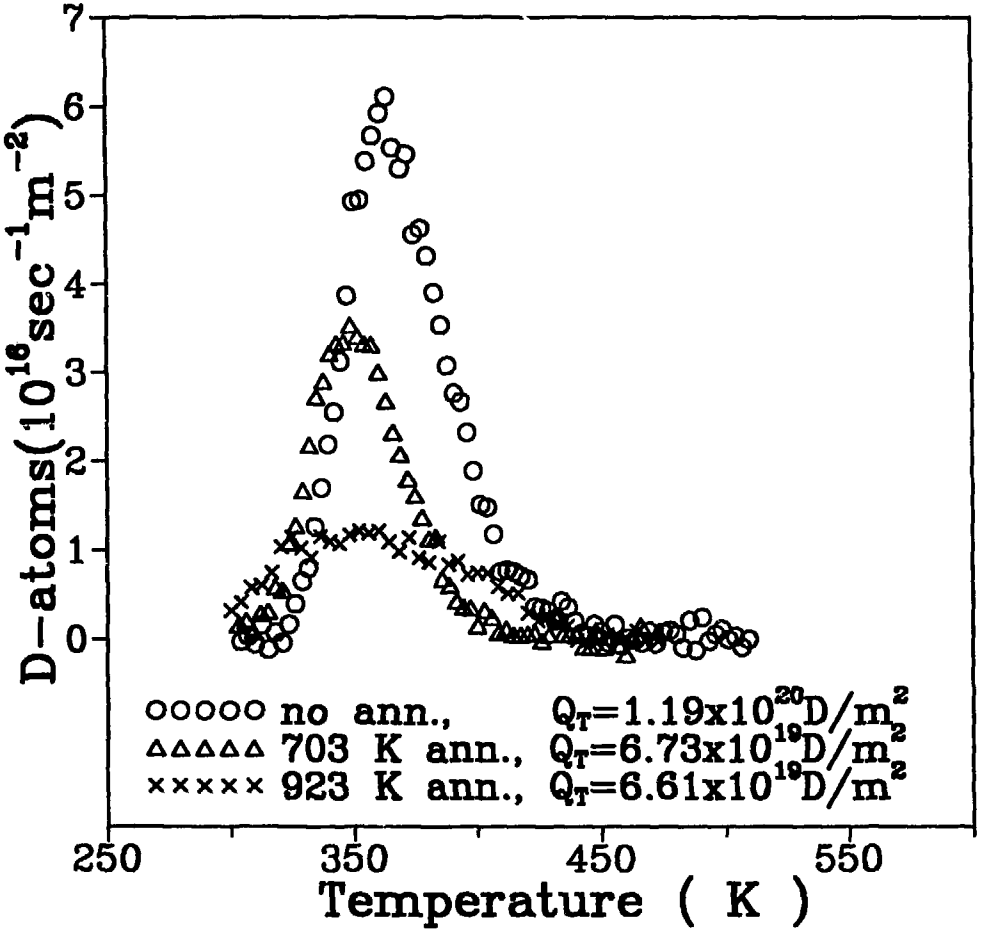
D−atoms(10^{16}sec^{-1}m^{-2})
7
6
5
4
3
2
1
0
250
350
450
550
Temperature (K)
○○○○○ no ann., Q_T=1.19x10^{20}D/m^2
△△△△△ 703 K ann., Q_T=6.73x10^{19}D/m^2
××××× 923 K ann., Q_T=6.61x10^{19}D/m^2

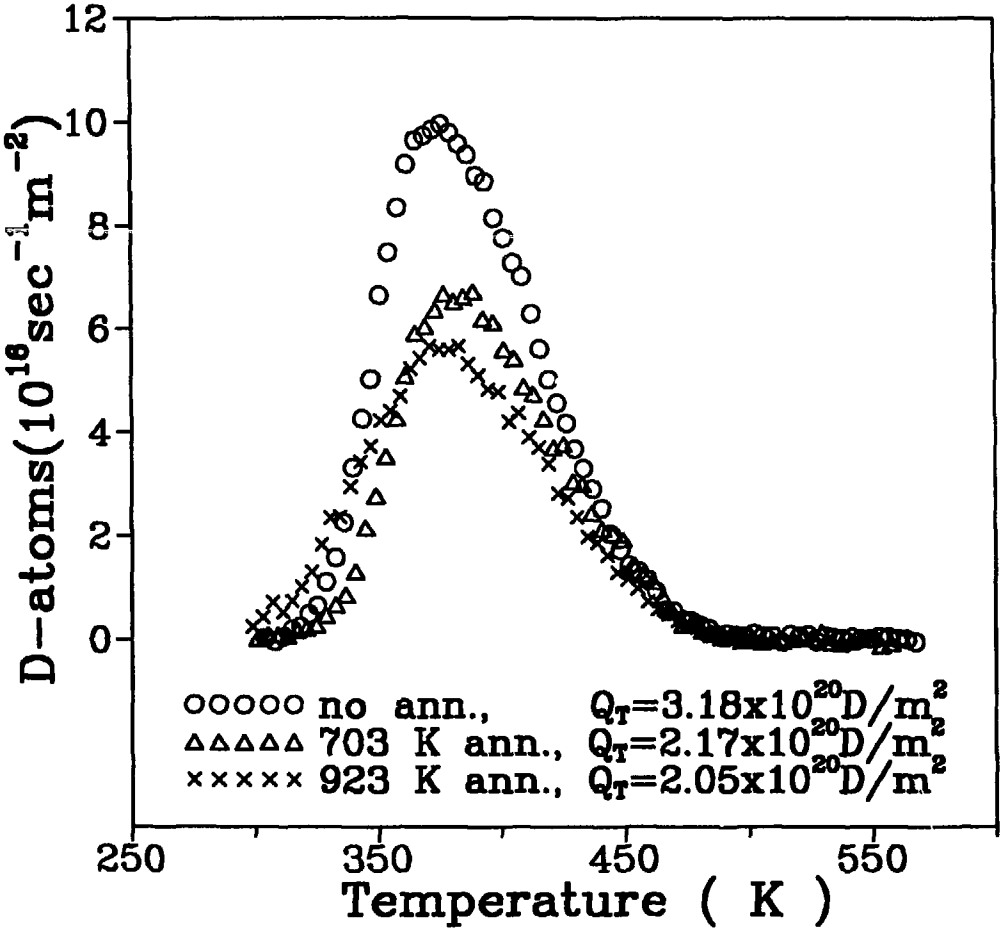
D−atoms(10^{16}sec^{-1}m^{-2})
12
10
8
6
4
2
0
250
350
450
550
Temperature (K)
○○○○○ no ann., Q_T=3.18x10^{20}D/m^2
△△△△△ 703 K ann., Q_T=2.17x10^{20}D/m^2
×××××× 923 K ann., Q_T=2.05x10^{20}D/m^2

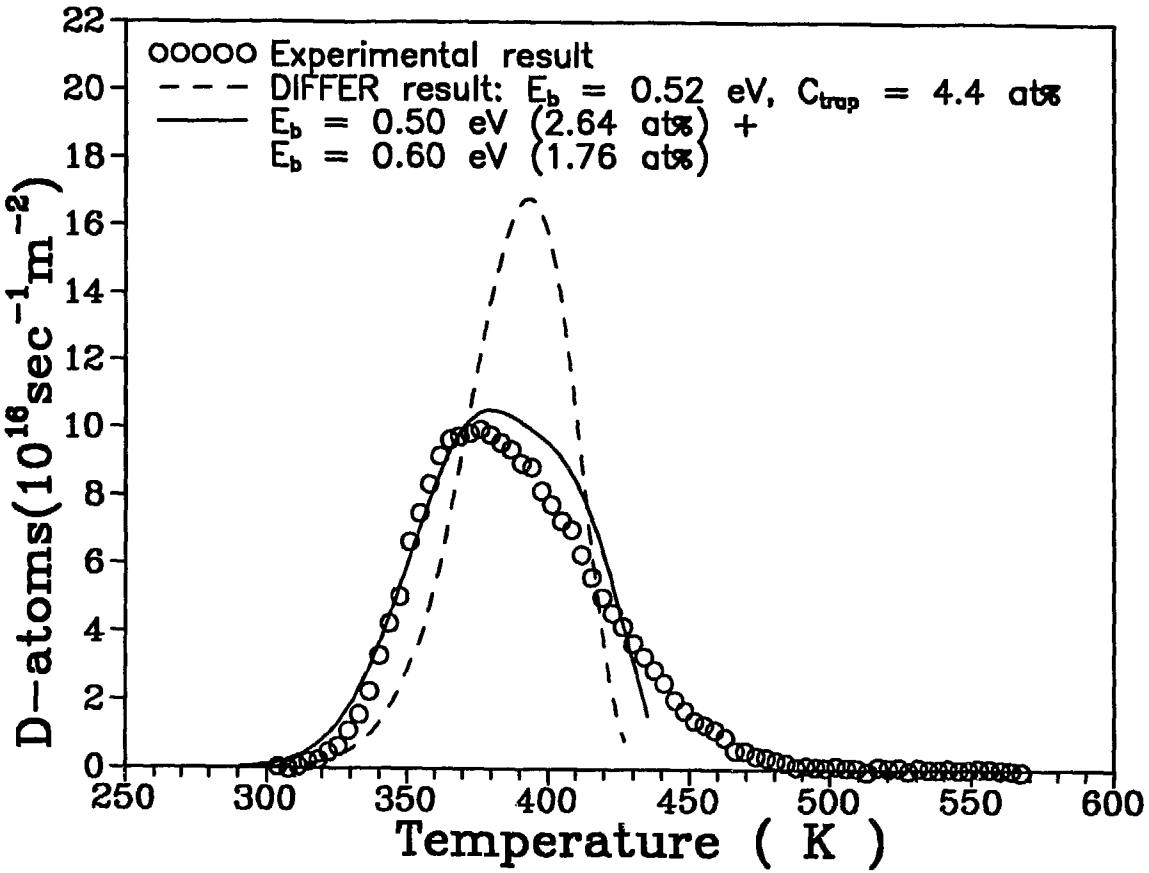
ooooo Experimental result
- - - DIFFER result: E_b = 0.52 eV, C_{trap} = 4.4 at%
——— E_b = 0.50 eV (2.64 at%) +
E_b = 0.60 eV (1.76 at%)
D-atoms(10^{16}sec^{-1}m^{-2})
Temperature (K)
0
2
4
6
8
10
12
14
16
18
20
22
250
300
350
400
450
500
550
600

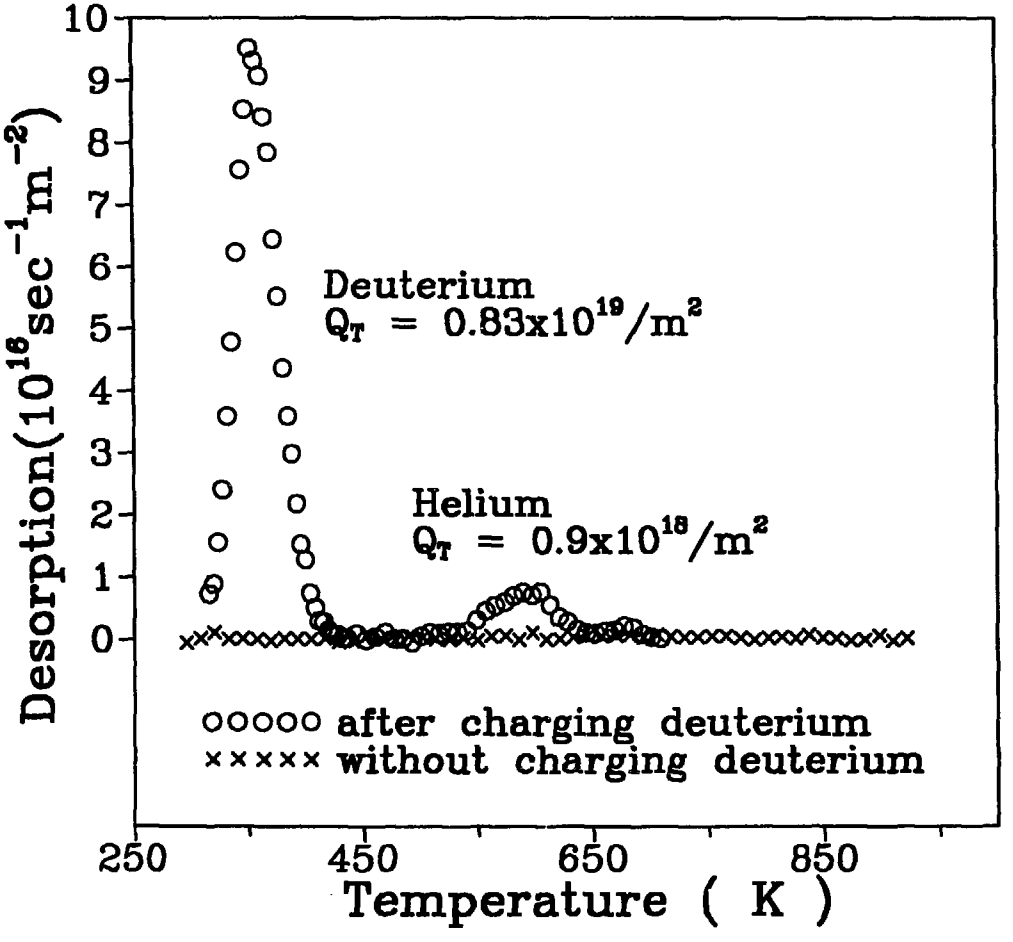
Desorption(10^{16}sec^{-1}m^{-2})
10
9
8
7
6
5
4
3
2
1
0
Deuterium
Q_T = 0.83x10^{19}/m^2
Helium
Q_T = 0.9x10^{18}/m^2
ooooo after charging deuterium
xxxxx without charging deuterium
250
450
650
850
Temperature (K)